arXiv:0804.2266v1 [astro-ph] 14 Apr 2008

INFLUENCE OF THE RELICT COSMOLOGICAL CONSTANT ON ACCRETION DISCS

ZDENĚK STUCHLÍK

Institute of Physics, Faculty of Philosophy and Science, Silesian University in Opava
Bezručovo nám. 13, CZ-746 01 Opava, Czech Republic
Zdenek.Stuchlik@fpf.slu.cz

Surprisingly, the relict cosmological constant has a crucial influence on properties of accretion discs orbiting black holes in quasars and active galactic nuclei. We show it by considering basic properties of both the geometrically thin and thick accretion discs in the Kerr–de Sitter black-hole (naked-singularity) spacetimes. Both thin and thick discs must have an outer edge allowing outflow of matter into the outer space, located nearby the so called static radius, where the gravitational attraction of a black hole is balanced by the cosmological repulsion. Jets produced by thick discs can be significantly collimated after crossing the static radius. Extension of discs in quasars is comparable with extension of the associated galaxies, indicating a possibility that the relict cosmological constant puts an upper limit on extension of galaxies.

1. Introduction

Recent data from a wide variety of independent cosmological tests indicate convincingly that within the framework of the inflationary cosmology a non-zero, although very small, vacuum energy density, i.e., a relict repulsive cosmological constant (RRCC), $\Lambda > 0$, or some kind of similarly acting quintessence, has to be invoked in order to explain the dynamics of the recent Universe.[1,2]

There is a strong "concordance" indication[3] that the observed value of the vacuum energy density is

$$\varrho_{\text{vac}(0)} \approx 0.73 \varrho_{\text{crit}(0)} \tag{1}$$

with present values of the critical energy density $\varrho_{\text{crit}(0)}$, and the Hubble parameter H_0 given by

$$\varrho_{\text{crit}(0)} = \frac{3H_0^2}{8\pi}, \quad H_0 = 100h \text{ km s}^{-1} \text{ Mpc}^{-1}. \tag{2}$$

2   *Z. Stuchlík*

Taking value of the dimensionless parameter $h \approx 0.7$, we obtain the RRCC to be

$$\Lambda_0 = 8\pi\varrho_{\text{vac}(0)} \approx 1.3 \times 10^{-56} \text{ cm}^{-2}. \tag{3}$$

It is well known that the RRCC strongly influences expansion of the Universe, leading finally to an exponentially accelerated stage.[4] However, surprisingly enough, the RRCC can be relevant for accretion processes in the field of central black holes in quasars and active galactic nuclei.

Basic properties of geometrically thin accretion discs with low accretion rates and negligible pressure are given by the circular geodetical motion in the black-hole backgrounds,[5] while for geometrically thick discs with high accretion rates and relevant pressure they are determined by equipotential surfaces of test perfect fluid rotating in the backgrounds.[6,7] The presence of the RRCC changes substantially the asymptotic structure of the black-hole (naked-singularity) backgrounds as they become asymptotically de Sitter and contain a cosmological event horizon behind which the spacetime is dynamic. Properties of the circular geodesic orbits in the Schwarzschild–de Sitter (SdS) and Reissner–Nordström–de Sitter (RNdS) spacetimes show that due to the presence of the RRCC, the thin discs have not only an inner edge determined (approximately) by the radius of the innermost stable circular orbit, but also an outer edge given by the radius of the outermost stable circular orbit, located nearby the static radius.[8,9] The vicinity of the static radius can be considered as a counterpart to the asymptotically flat region of the Kerr spacetimes, as can be demonstrated by the embedding diagrams of the equatorial plane of both the directly projected geometry and the optical reference geometry reflecting some hidden properties of the geodesic motion.[10,11,12] The analysis of equilibrium configurations of perfect fluid orbiting in the SdS black-hole backgrounds shows a possible existence of thick discs with outflow of matter through an outer cusp of the equilibrium configuration due to violation of mechanical equilibrium.[13] Such an outflow can represent a strong stabilizing effect[14] against the runaway instability[15] of thick discs orbiting the SdS black holes.

However, it is crucial to understand the role of the RRCC in astrophysically most relevant, rotating Kerr backgrounds. In the Kerr–de Sitter (KdS) backgrounds, we shall consider circular equatorial motion of test particles, relevant for thin discs, and equilibrium configurations of perfect fluid, relevant for thick discs. We shall focus attention on the black-hole backgrounds, but some results related to the naked-singularity backgrounds will be mentioned because of increasing theoretical evidence on possible existence of naked singularities.[16]

2. Kerr–de Sitter spacetimes

In the standard Boyer–Lindquist coordinates (t, r, θ, ϕ) and the geometric units $(c = G = 1)$, the Kerr–(anti-)de Sitter geometry is given by the line element

$$ds^2 = -\frac{\Delta_r}{I^2\rho^2}(dt - a\sin^2\theta d\phi)^2 + \frac{\Delta_\theta \sin^2\theta}{I^2\rho^2}\left[adt - \left(r^2 + a^2\right)d\phi\right]^2$$
$$+ \frac{\rho^2}{\Delta_r}dr^2 + \frac{\rho^2}{\Delta_\theta}d\theta^2, \tag{4}$$

where

$$\Delta_r = -\frac{1}{3}\Lambda r^2\left(r^2 + a^2\right) + r^2 - 2Mr + a^2, \tag{5}$$

$$\Delta_\theta = 1 + \frac{1}{3}\Lambda a^2\cos^2\theta, \quad I = 1 + \frac{1}{3}\Lambda a^2, \quad \rho^2 = r^2 + a^2\cos^2\theta. \tag{6}$$

The parameters of the spacetime are: mass (M), specific angular momentum (a), cosmological constant (Λ). It is convenient to introduce a dimensionless cosmological parameter

$$y = \frac{1}{3}\Lambda M^2. \tag{7}$$

For simplicity, we put $M = 1$ hereafter. Equivalently, also the coordinates t, r, the line element ds, and the rotational parameter of the spacetime a, being expressed in units of M, become dimensionless. We focus our attention to the case $y > 0$ corresponding to the repulsive cosmological constant; then (4) describes a KdS spacetime.

The event horizons of the spacetime are given by the pseudosingularities of the line element (4), determined by the condition $\Delta_r = 0$. The loci of the event horizons are implicitly determined by the relation

$$a^2 = a_{\mathrm{h}}^2(r;y) \equiv \frac{r^2 - 2r - yr^4}{yr^2 - 1}. \tag{8}$$

It can be shown[17] that a critical value of the cosmological parameter exists

$$y_{\mathrm{c(KdS)}} = \frac{16}{(3 + 2\sqrt{3})^3} \doteq 0,05924, \tag{9}$$

such that for $y > y_{\mathrm{c(KdS)}}$, only naked-singularity backgrounds exist for $a^2 > 0$. There is another critical value $y_{\mathrm{c(SdS)}} = 1/27 \doteq 0.03704$, which is limiting the existence of SdS black holes.[8] In the RNdS spacetimes, the critical value is[9] $y_{\mathrm{c(RNdS)}} = 2/27 \doteq 0.07407$.

If $y = y_{\mathrm{c(KdS)}}$, the function $a_{\mathrm{h}}^2(r;y)$ has an inflex point corresponding to a critical value of the rotation parameter of the KdS spacetimes

$$a_{\mathrm{crit}}^2 = \frac{3}{16}(3 + 2\sqrt{3}) \doteq 1,21202. \tag{10}$$

KdS black holes can exist for $a^2 < a_{\mathrm{crit}}^2$ only, while KdS naked singularities can exist for both $a^2 < a_{\mathrm{crit}}^2$ and $a^2 > a_{\mathrm{crit}}^2$.

Separation of the KdS black-hole and naked-singularity spacetimes in the parameter space y–a^2 is shown in Fig. 1. In the black-hole spacetimes there are two
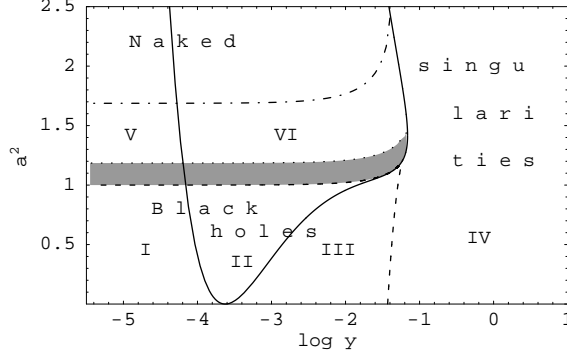
4   *Z. Stuchlík*

Fig. 1.   Classification of the Kerr–de Sitter spacetimes. Dashed curves separate black holes and naked singularities. Full curves divide the parametric space by properties of the stable circular orbits relevant for Keplerian accretion discs. Spacetimes with both plus-family and minus-family stable circular orbits (**I** and **V**). Spacetimes with no minus-family stable circular orbits (**II** and **VI**). Spacetimes with no stable circular orbits (**III** and **IV**). Dashed-dotted curve defines the subregion of the naked-singularity spacetimes, where the plus-family circular orbits could be stable and counter-rotating (from the point of view of the LNRF), shaded is the subregion allowing stable circular orbits with $E_+ < 0$! (Taken from Ref. 17.)

black-hole horizons and the cosmological horizon, with $r_{h-} < r_{h+} < r_c$. In the naked-singularity spacetimes, there is the cosmological horizon r_c only.

The extreme cases, when two (or all three) horizons coalesce, were discussed in detail for the case of RNdS spacetimes.[18,19] In the KdS spacetimes, the situation is analogical. If $r_{h-} = r_{h+} < r_c$, the extreme black-hole case occurs, if $r_{h-} < r_{h+} = r_c$, the marginal naked-singularity case occurs, if $r_{h-} = r_{h+} = r_c$, the "ultra-extreme" case occurs corresponding to a naked singularity.

3. Thin discs

Basic properties of thin accretion discs are determined by equatorial circular motion of test particles because any tilted disc has to be driven to the equatorial plane of the rotating spacetimes due to the dragging of inertial frames.[20]

The motion of a test particle with rest mass m is given by the geodesic equations. In a separated and integrated form, the equations were obtained by Carter.[21] For the motion restricted to the equatorial plane ($\mathrm{d}\theta/\mathrm{d}\lambda = 0$, $\theta = \pi/2$) of the KdS spacetime, the Carter equations take the following form

$$r^2 \frac{\mathrm{d}r}{\mathrm{d}\lambda} = \pm R^{1/2}(r), \tag{11}$$

$$r^2 \frac{\mathrm{d}\phi}{\mathrm{d}\lambda} = -IP_\theta + \frac{aIP_r}{\Delta_r}, \tag{12}$$

$$r^2 \frac{\mathrm{d}t}{\mathrm{d}\lambda} = -aIP_\theta + \frac{(r^2 + a^2)IP_r}{\Delta_r}, \tag{13}$$

where

$$R(r) = P_r^2 - \Delta_r \left(m^2 r^2 + K\right), \tag{14}$$

$$P_r = I\mathcal{E}\left(r^2 + a^2\right) - Ia\Phi, \quad P_\theta = I(a\mathcal{E} - \Phi), \quad K = I^2(a\mathcal{E} - \Phi)^2. \tag{15}$$

The proper time of the particle τ is related to the affine parameter λ by $\tau = m\lambda$. The constants of motion are: energy $(\mathcal{E})$, related to the stationarity of the geometry, axial angular momentum (Φ), related to the axial symmetry of the geometry, 'total' angular momentum (K), related to the hidden symmetry of the geometry. For the equatorial motion, K is restricted through Eq. (15) following from the conditions on the latitudinal motion.[22] Notice that $\mathcal{E}$ and Φ cannot be interpreted as energy and axial angular momentum at infinity, since the spacetime is not asymptotically flat.

The equatorial motion is governed by the constants of motion $\mathcal{E}$, Φ. Its properties can be conveniently determined by an "effective potential" given by the condition $R(r) = 0$ for turning points of the radial motion. It is useful to define specific energy and specific angular momentum by the relations

$$E \equiv \frac{I\mathcal{E}}{m}, \; L \equiv \frac{I\Phi}{m}. \tag{16}$$

Solving the equation $R(r) = 0$, we find the effective potential in the form

$$E_{(\pm)}(r; L, a, y) \equiv \left[\left(1 + ya^2\right) r \left(r^2 + a^2\right) + 2a^2\right]^{-1}$$
$$\times \left\{ a \left[yr \left(r^2 + a^2\right) + 2\right] L \right.$$
$$\left. \pm \Delta_r^{1/2} \left\{r^2 L^2 + r \left[\left(1 + ya^2\right) r \left(r^2 + a^2\right) + 2a^2\right]\right\}^{1/2}\right\}. \tag{17}$$

In the stationary regions $(\Delta_r \geq 0)$, the motion is allowed where[23]

$$E \geq E_{(+)}(r; L, a, y). \tag{18}$$

The equatorial circular orbits can be determined by solving simultaneously the equations $R(r) = 0, dR/dr = 0$. The specific energy of the orbits is given by

$$E_\pm(r; a, y) = \frac{1 - \frac{2}{r} - \left(r^2 + a^2\right) y \pm a \left(\frac{1}{r^3} - y\right)^{1/2}}{\left[1 - \frac{3}{r} - a^2 y \pm 2a \left(\frac{1}{r^3} - y\right)^{1/2}\right]^{1/2}}, \tag{19}$$

while the specific angular momentum of the orbits is determined by

$$L_\pm(r; a, y) = -\frac{2a + ar \left(r^2 + a^2\right) y \mp r \left(r^2 + a^2\right) \left(\frac{1}{r^3} - y\right)^{1/2}}{r \left[1 - \frac{3}{r} - a^2 y \pm 2a \left(\frac{1}{r^3} - y\right)^{1/2}\right]^{1/2}}. \tag{20}$$

The relations (19)–(20) determine two families of the circular orbits. We call them plus-family orbits and minus-family orbits[17] according to the $\pm$ sign in the relations

6 *Z. Stuchlík*

(19)–(20). Inspecting expressions (19) and (20), we find two reality restrictions on the circular orbits. The first one is given by the relation

$$y \leq y_{\rm s} \equiv \frac{1}{r^3}, \tag{21}$$

which introduces the notion of the "static radius", given by the formula $r_{\rm s} = y^{-1/3}$ independently of the rotational parameter a. It can be compared with formally identical result in the Schwarzschild–de Sitter spacetimes.[8] A "free" or "geodetical" observer on the static radius has only U^t component of 4-velocity being non-zero. The position on the static radius is unstable relative to radial perturbations. The second restriction is given by the condition

$$1 - \frac{3}{r} - a^2 y \pm 2a \left(\frac{1}{r^3} - y \right)^{1/2} \geq 0; \tag{22}$$

the equality determines photon circular orbits with $E \to \infty$ and $L \to \pm\infty$. The photon circular orbits of the plus-family are given by the relation

$$a = a_{\rm ph(1,2)}^{(+)}(r;y) \equiv \frac{\left(1 - yr^3 \right)^{1/2} \pm \left(1 - 3yr^2 \right)^{1/2}}{yr^{3/2}}, \tag{23}$$

while for the minus-family orbits they are given by

$$a = a_{\rm ph(1,2)}^{(-)}(r;y) \equiv \frac{-\left(1 - yr^3 \right)^{1/2} \pm \left(1 - 3yr^2 \right)^{1/2}}{yr^{3/2}}. \tag{24}$$

A detailed discussion of the photon circular orbits can be found in Refs. 11, 17.

The behaviour of circular orbits in the field of Kerr black holes ($y = 0$) suggests that the plus-family orbits correspond to the co-rotating orbits, while the minus-family circular orbits correspond to the counter-rotating ones. However, this statement is not correct even for Kerr naked-singularity spacetimes with the rotational parameter low enough, where counter-rotating plus-family orbits could exist nearby the ring singularity.[24] In the KdS spacetimes we cannot identify the plus-family circular orbits with purely co-rotating orbits even in the black-hole spacetimes; moreover, it is not possible to define the co-rotating (counter-rotating) orbits in relation to stationary observers at infinity, as can be done in the Kerr spacetimes, since the KdS spacetimes are not asymptotically flat.

Orientation of the circular orbits in the KdS spacetimes must be related to locally non-rotating frames (LNRF), similarly to the case of asymptotically flat Kerr spacetimes. In the KdS spacetimes, the tetrad of 1-forms corresponding to the LNRF is given by Ref. 11:

$$\omega^{(t)} \equiv \left(\frac{\Delta_r \Delta_\theta \varrho^2}{I^2 A} \right)^{1/2} {\rm d}t, \qquad \omega^{(\phi)} \equiv \left(\frac{A \sin^2 \theta}{I^2 \varrho^2} \right)^{1/2} ({\rm d}\phi - \Omega {\rm d}t), \tag{25}$$

$$\omega^{(r)} \equiv \left(\frac{\varrho^2}{\Delta_r} \right)^{1/2} {\rm d}r, \qquad \omega^{(\theta)} \equiv \left(\frac{\varrho^2}{\Delta_\theta} \right)^{1/2} {\rm d}\theta, \tag{26}$$

with the angular velocity of the LNRF being given by

$$\Omega \equiv \frac{\mathrm{d}\phi}{\mathrm{d}t} = \frac{a}{A}\left[-\Delta_r + (r^2 + a^2)\Delta_\theta\right]; \quad A \equiv (r^2 + a^2)^2 - a^2\Delta_r. \tag{27}$$

Locally measured components of 4-momentum in the LNRF are given by the projection of a particle's 4-momentum onto the tetrad

$$p^{(\alpha)} = p^\mu \omega_\mu^{(\alpha)}, \quad p^\mu = m\frac{\mathrm{d}x^\mu}{\mathrm{d}\tau} \equiv m\dot{x}^\mu = \frac{\mathrm{d}x^\mu}{\mathrm{d}\lambda}. \tag{28}$$

A simple calculation reveals the intuitively anticipated relation

$$p^{(\phi)} = \frac{mr}{A^{1/2}}L. \tag{29}$$

We can see that the sign of the azimuthal component of the 4-momentum measured in the LNRF is given by the sign of the specific angular momentum of a particle on the orbit of interest. Therefore the circular orbits with $p^{(\phi)} > 0$, $(L > 0)$, we call co-rotating, and the circular orbits with $p^{(\phi)} < 0$, $(L < 0)$ we call counter-rotating, in agreement with the case of asymptotically flat Kerr spacetimes.

The circular geodesics can be astrophysically relevant, if they are stable with respect to radial perturbations. The loci of the stable circular orbits are given by the condition

$$\frac{\mathrm{d}^2 R}{\mathrm{d}r^2} \geq 0 \tag{30}$$

that has to be satisfied simultaneously with the conditions $R(r) = 0$ and $\mathrm{d}R/\mathrm{d}r = 0$ determining the circular orbits. The radii of the stable orbits of both families are restricted by the condition[17]

$$r\left[6 - r + r^3(4r - 15)y\right] \mp 8a\left[r\left(1 - yr^3\right)^3\right]^{1/2} + a^2\left[3 + r^2 y\left(1 - 4yr^3\right)\right] \geq 0. \tag{31}$$

The marginally stable orbits of both families are described by the relation

$$a^2 = a_{\mathrm{ms}(1,2)}^2(r; y) \equiv \left[3 + r^2 y\left(1 - 4yr^3\right)\right]^{-2} r\Bigg\{ \left[r - 6 - r^3(4r - 15)y\right]$$
$$\times \left[3 + r^2 y\left(1 - 4yr^3\right)\right] + 32\left(1 - yr^3\right)^3 \pm 8\left(1 - yr^3\right)^{3/2}\left(1 - 4yr^3\right)^{1/2}$$
$$\times \left\{r\left[3 - ry\left(6 + 10r - 15yr^3\right)\right] - 2\right\}^{1/2}\Bigg\}. \tag{32}$$

The $(\pm)$ sign in Eq. (32) is not directly related to the plus-family and the minus-family orbits. The function $a_{\mathrm{ms}(1)}^2$, corresponding to the $(+)$ sign in Eq. (32), determines marginally stable orbits of the plus-family, while the function $a_{\mathrm{ms}(2)}^2$, corresponding to the $(-)$ sign in Eq. (32), is relevant for both the plus-family and minus-family orbits. A detailed analysis shows that the critical value of the cosmological parameter for the existence of the stable (plus-family) orbits is given by

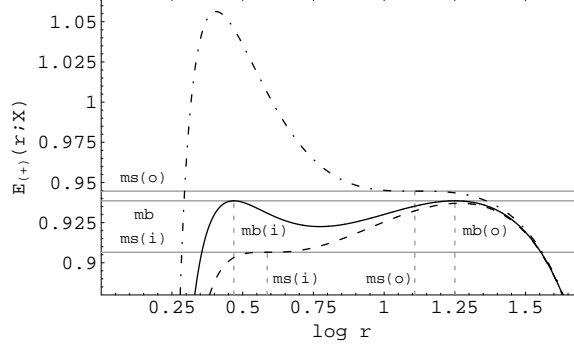$$y_{\mathrm{crit(ms+)}} = \frac{100}{(5 + 2\sqrt{10})^3} \doteq 0.06886. \tag{33}$$

Fig. 2.   Effective potentials of equatorial radial motion of test particles in Kerr–de Sitter black-hole spacetime ($y = 10^{-4}$, $a = 0.6$) allowing stable circular orbits for co-rotating particles. Marginally bound (mb) orbits are given by the solid curve corresponding to $X = X_{mb+} \doteq 2.38445$. The curve has two local maxima of the same value, $E_{mb} \doteq 0.93856$, leading to inner (mb(i)) and outer (mb(o)) marginally bound orbits. The dashed effective potential defines inner marginally stable orbit (ms(i)) by coalescing local minimum and (inner) local maximum, and corresponds to $X = X_{ms(i)+} \doteq 2.20307$ with energy $E_{ms(i)+} \doteq 0.90654$. In an analogous manner the dashed-dotted potential defines outer marginally stable orbit (ms(o)) with energy $E_{ms(o)+} \doteq 0.94451$ corresponding to $X = X_{ms(o)+} \doteq 2.90538$. (Taken from Ref. 17.)

No stable circular orbits (of any family) exist for $y > y_{\text{crit(ms+)}}$. The critical value of y for the existence of the minus-family stable circular orbits is given by

$$y_{\text{crit(ms-)}} = \frac{12}{15^4}. \tag{34}$$

It coincides with the limit on the existence of the stable circular orbits in the SdS spacetimes.[8] In the parameter space y–a^2, separation of the KdS spacetimes according to the existence of stable circular orbits is given in Fig. 1.

Behaviour of the effective potential (17) enables us to introduce the notion of marginally bound orbits, i.e., unstable circular orbits where a small radial perturbation causes infall of a particle from the orbit to the centre, or its escape to the cosmological horizon. For some special value of the axial parameter $X = L - aE$, denoted as X_{mb}, the effective potential has two local maxima related by

$$E_{(+)}(r_{\text{mb(i)}}; X_{\text{mb}}, a, y) = E_{(+)}(r_{\text{mb(o)}}; X_{\text{mb}}, a, y), \tag{35}$$

corresponding to both the inner and outer marginally bound orbits, see Fig. 2. For completeness, the figure includes the effective potentials defining both the inner and outer marginally stable orbits. The search for the marginally bound orbits in a concrete KdS spacetime admitting stable circular orbits must be realized in a numerical way. Clearly, in the spacetimes with $y \geq 12/15^4$, the minus-family marginally bound orbits do not exist. In the spacetimes admitting stable plus-family orbits, there is $r_{\text{mb(o)}} \sim r_{\text{s}}$ but $r_{\text{ms(o)}} \sim 0.7 r_{\text{s}}$.

In comparison with the asymptotically flat Kerr spacetimes, where the effect of spacetime rotation vanishes for asymptotically large values of the radius, in the

KdS spacetimes the properties of the circular orbits must be treated more carefully, because the rotational effect is relevant in the whole region where the circular orbits are allowed and it survives even at the cosmological horizon.

The minus-family orbits have $L_- < 0$ in each KdS spacetime and such orbits are counter-rotating relative to the LNRF.

In the black-hole spacetimes, the plus-family orbits are co-rotating in almost all radii where the circular orbits are allowed except some region in vicinity of the static radius, where they become to be counter-rotating. However, these orbits are unstable. The specific angular momentum and energy of particles located at the static radius, where the plus-family and minus-family orbits coalesce, are given by

$$L_{\rm s} = -a \frac{3y^{1/3} + a^2 y}{\left(1 - 3y^{1/3} - a^2 y\right)^{1/2}}, \quad E_{\rm s} = (1 - 3y^{1/3} - a^2 y)^{1/2}. \tag{36}$$

In the naked-singularity spacetimes, the plus-family orbits behave in a more complex way. They are always counter-rotating in vicinity of the static radius. Moreover, in the naked singularity spacetimes with the rotational parameter low enough ($a < 3\sqrt{3}/4$, $y = 0$), stable counter-rotating plus-family circular orbits exist. When a is very close to the extreme hole state ($a < 4\sqrt{2}/(3\sqrt{3})$, $y = 0$), even stable plus-family orbits with $E < 0$ can exist,[17] see Fig. 1.

Angular velocity $\Omega = {\rm d}\phi/{\rm d}t$ of a thin, Keplerian accretion disc is given by

$$\Omega_{\rm K\pm} = \pm \frac{1}{r^{3/2}/(1 - yr^3)^{1/2} \pm a}. \tag{37}$$

Matter in the thin disc spirals from the outer marginally stable orbit through the sequence of stable circular orbits down to the inner marginally stable orbit losing energy and angular momentum due to the viscosity. The necessary conditions for such a differential rotation

$$\frac{{\rm d}\Omega_{\rm K+}}{{\rm d}r} < 0 \quad \frac{{\rm d}L_+}{{\rm d}r} \geq 0 \qquad \text{or} \qquad \frac{{\rm d}\Omega_{\rm K-}}{{\rm d}r} > 0 \quad \frac{{\rm d}L_-}{{\rm d}r} \leq 0, \tag{38}$$

are fulfilled by the relations (20) and (37). The efficiency of accretion, i.e., the efficiency of conversion of rest mass into heat energy of any element of matter transversing the discs from their outer edge located on the outer marginally stable orbit to their inner edge located on the inner marginally stable orbit is given by

$$\eta \equiv E_{\rm ms(o)} - E_{\rm ms(i)}. \tag{39}$$

For Keplerian discs co-rotating extreme KdS black holes, the accretion efficiency reaches maximum value of $\eta \sim 0.43$ for the pure Kerr case ($y = 0$) and tends to zero for $y \to y_{\rm c(KdS)} \doteq 0.059$, the maximum value of y admitting black holes[a].

---

[a]Notice that for the plus-family discs orbiting Kerr naked singularities with $a \sim 1$, the efficiency $\eta \sim 1.57$, exceeding strongly the annihilation efficiency. This is caused by strong discontinuity in properties of the plus-family orbits for extreme black holes and naked singularities with $a \to 1$. Conversion of a naked singularity into an extreme black hole leads to an abrupt instability of the innermost parts of the plus-family discs that can have strong observational consequences.[17]

10 *Z. Stuchlík*

4. Thick discs

Basic properties of thick discs are determined by equilibrium configurations of perfect fluid. Stress-energy tensor of perfect fluid is given by

$$T^{\mu}{}_{\nu} = (p + \epsilon)U^{\mu}U_{\nu} + p\,\delta^{\mu}_{\nu} \tag{40}$$

where ϵ and p denote total energy density and pressure of the fluid, U^{μ} is its four velocity. We shall consider test perfect fluid rotating in the ϕ direction, i.e., $U^{\mu} = \left(U^{t}, U^{\phi}, 0, 0\right)$. The rotating fluid can be characterized by the vector fields of the angular velocity $\Omega\,(r, \theta)$ and the angular momentum density $\ell\,(r, \theta)$, defined by

$$\Omega = \frac{U^{\phi}}{U^{t}}, \qquad \ell = -\frac{U_{\phi}}{U_{t}}. \tag{41}$$

The vector fields are related by the metric coefficients of the KdS spacetime

$$\Omega = -\frac{g_{t\phi} + \ell g_{tt}}{g_{\phi\phi} + \ell g_{t\phi}}. \tag{42}$$

Projecting the energy-momentum conservation law $T^{\mu\nu}{}_{;\nu} = 0$ onto the hypersurface orthogonal to the four velocity U^{μ} by the projection tensor $h_{\mu\nu} = g_{\mu\nu} + U_{\mu}U_{\nu}$, we obtain the relativistic Euler equation in the form

$$\frac{\partial_{\mu}p}{p + \epsilon} = -\partial_{\mu}(\ln U_{t}) + \frac{\Omega\,\partial_{\mu}\ell}{1 - \Omega\ell}, \tag{43}$$

where

$$(U_{t})^{2} = \frac{g_{t\phi}^{2} - g_{tt}\,g_{\phi\phi}}{g_{\phi\phi} + 2\ell g_{t\phi} + \ell^{2}g_{tt}}. \tag{44}$$

For barytropic perfect fluid, i.e., the fluid with an equation of state $p = p(\epsilon)$, the solution of the relativistic Euler equation can be given by Boyer's condition determining the surfaces of constant pressure through the "equipotential surfaces" of the potential $W(r, \theta)$ by the relations[7]

$$\int_{0}^{p} \frac{\mathrm{d}p}{p + \epsilon} = W_{\mathrm{in}} - W = \ln(U_{t})_{\mathrm{in}} - \ln(U_{t}) + \int_{\ell_{\mathrm{in}}}^{\ell} \frac{\Omega\,\mathrm{d}\ell}{1 - \Omega\ell}; \tag{45}$$

the subscript "in" refers to the inner edge of the disc.

The equipotential surfaces are determined by the condition

$$W(r, \theta) = \mathrm{const}, \tag{46}$$

and in a given spacetime can be found from Eq. (45), if a rotation law $\Omega = \Omega(\ell)$ is given. Equilibrium configurations of test perfect fluid are determined by the equipotential surfaces which can be closed or open. Moreover, there is a special class of critical, self-crossing surfaces (with a cusp), which can be either closed or open. The closed equipotential surfaces determine stationary toroidal configurations. The fluid can fill any closed surface – at the surface of the equilibrium configuration pressure vanishes, but its gradient is non-zero.[6] On the other hand, the open equipotential surfaces are important in dynamical situations, *e.g.*, in modeling of jets.[25,26] The

critical, self-crossing closed equipotential surfaces W_{cusp} are important in the theory of thick accretion discs, because accretion onto the black hole through the cusp of the equipotential surface, located in the equatorial plane, is possible due to a little overcoming of the critical equipotential surface by the surface of the disc (Paczyński mechanism). Accretion is thus driven by a violation of the hydrostatic equilibrium, rather than by viscosity of the accreting matter.[6]

It is well known that all characteristic properties of the equipotential surfaces for a general rotation law are reflected by the equipotential surfaces of the simplest configurations with uniform distribution of the angular momentum density ℓ, see Ref. 27. Moreover, these configurations are very important astrophysically, because they are marginally stable.[28] Under the condition

$$\ell(r,\theta) = \mathrm{const}, \tag{47}$$

a simple relation for the equipotential surfaces follows from Eq. (45):

$$W(r,\theta) = \ln U_t(r,\theta). \tag{48}$$

The equipotential surfaces $\theta = \theta(r)$ are given by the relation

$$\frac{\mathrm{d}\theta}{\mathrm{d}r} = -\frac{\partial p/\partial r}{\partial p/\partial \theta}, \tag{49}$$

which for the configurations with $\ell = \mathrm{const}$ reduces to

$$\frac{\mathrm{d}\theta}{\mathrm{d}r} = -\frac{\partial U_t/\partial r}{\partial U_t/\partial \theta}. \tag{50}$$

In the KdS spacetimes there is

$$W(r,\theta) = \ln\left\{\frac{\rho}{I} \cdot \frac{\Delta_r^{1/2}\Delta_\theta^{1/2}\sin\theta}{\left[\Delta_\theta\sin^2\theta\left(r^2 + a^2 - a\ell\right)^2 - \Delta_r\left(\ell - a\sin^2\theta\right)^2\right]^{1/2}}\right\}. \tag{51}$$

The best insight into the $\ell = \mathrm{const}$ configurations is given by properties of $W(r,\theta)$ in the equatorial plane ($\theta = \pi/2$). The reality conditions of $W(r,\theta = \pi/2)$ imply

$$\ell_{\mathrm{ph}-} < \ell < \ell_{\mathrm{ph}+}, \tag{52}$$

where the functions $\ell_{\mathrm{ph}\pm}(r;a,y)$, given by

$$\ell_{\mathrm{ph}\pm}(r;a,y) = a + \frac{r^2}{a \pm \sqrt{\Delta_r}}, \tag{53}$$

determine the photon geodesic motion.[11,17]

Condition for the local extrema of the potential $W(r,\theta = \pi/2)$ is identical with the condition of vanishing of the pressure gradient ($\partial U_t/\partial r = 0 = \partial U_t/\partial \theta$). Since in the equatorial plane there is $\partial U_t/\partial \theta = 0$, independently of $\ell = \mathrm{const}$, the only relevant condition is $\partial U_t/\partial r = 0$, which implies the relation

$$\ell = \ell_{\mathrm{K}\pm}(r;a,y) \tag{54}$$
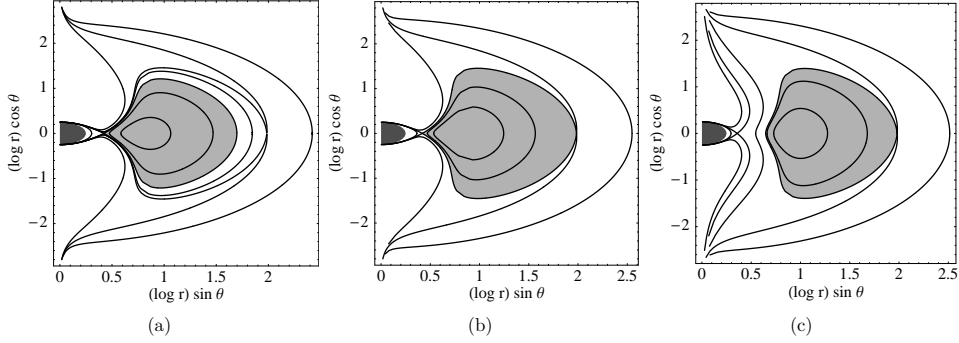
12   *Z. Stuchlík*

Fig. 3.   Typical behaviour of equipotential surfaces (meridional sections) in the KdS black-hole spacetimes. Light gray region contains closed equipotential surfaces. The last closed surface is self-crossing in the cusp(s). Possible toroidal configurations correspond to: (a) accretion discs, (b) marginally bound accretion discs and (c) excretion discs.

with $\ell_{\mathrm{K}\pm}$ being the angular momentum density of the geodetical Keplerian orbits

$$\ell_{\mathrm{K}\pm}(r;a,y) \equiv \pm \frac{(r^2+a^2)(1-yr^3)^{1/2} \mp ar^{1/2}[2+yr(r^2+a^2)]}{r^{3/2}[1-y(r^2+a^2)]-2r^{1/2}\pm a(1-yr^3)^{1/2}}. \tag{55}$$

The closed equipotential surfaces, and surfaces with a cusp allowing the outflow of matter from the disc, are permitted in those parts of the functions $\ell_{\mathrm{K}\pm}(r;a,y)$ enabling the existence of stable circular geodesics corresponding to the centre of the equilibrium configurations. Stationary toroidal configurations exist if $\ell \in (\ell_{\mathrm{ms(i)}}, \ell_{\mathrm{ms(o)}})$. We can distinguish three kinds of discs (Fig. 3):

accretion discs: $\ell \in (\ell_{\mathrm{ms(i)}}, \ell_{\mathrm{mb}})$; the last closed surface is self-crossing in the inner cusp, another critical surface self-crossing in the outer cusp is open.

marginally bound accretion discs: $\ell = \ell_{\mathrm{mb}}$; the last closed surface is self-crossing in both the inner and the outer cusp.

excretion discs: $\ell \in (\ell_{\mathrm{mb}}, \ell_{\mathrm{ms(o)}})$; the last closed surface is self-crossing in the outer cusp, another critical surface self-crossing in the inner cusp is open.

5. Conclusions

For astrophysically relevant black holes ($M < 10^{12} M_\odot$) and the observed RRCC (3), the cosmological parameter is so small ($y < 10^{-22}$) that both co-rotating and counter-rotating discs can exist around KdS black holes. The efficiency of the accretion process is then extremely close to the values relevant for Kerr black holes. The efficiency is strongest for thin, Keplerian discs orbiting extreme black holes. It is suppressed for a descending and/or for $\ell =$ const growing from $\ell_{\mathrm{ms(i)}}$ up to ℓ_{mb}. Notice that the co-rotating toroidal discs are steeper and more extended than the counter-rotating discs.

   The crucial effects caused by the RRCC are illustrated in (Fig. 4).
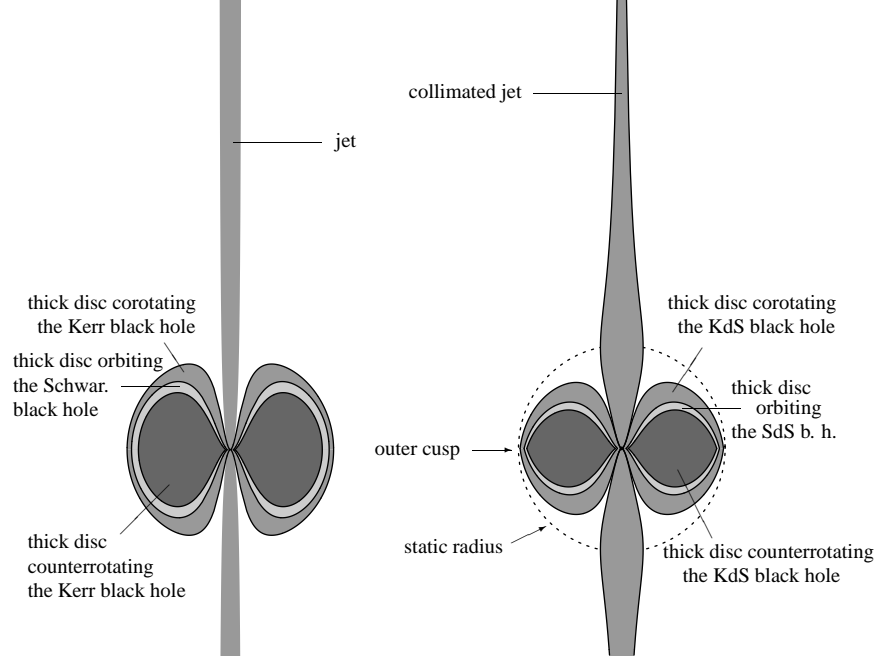
Fig. 4.   Shapes of thick discs and collimation of jets due to a cosmic repulsion. The effect of collimation is relevant near the static radius and further. Left picture depicts thick accretion discs orbiting the Kerr black hole ($y = 0$, $a^2 = 0.99$; $\ell \approx \ell_{\mathrm{mb}}$) and the Schwarzschild black hole ($y = 0$, $a = 0$; $\ell \approx \ell_{\mathrm{mb}}$), right picture depicts thick marginally bound accretion discs orbiting the KdS black hole ($y = 10^{-6}$, $a^2 = 0.99$; $\ell = \ell_{\mathrm{mb}}$) and the SdS black hole ($y = 10^{-6}$, $a = 0$; $\ell = \ell_{\mathrm{mb}}$).

- The outer edge of the discs. The presence of an outer cusp of toroidal discs nearby the static radius enables outflow of mass and angular momentum from the discs due to a violation of mechanical equilibrium. Recall that such an outflow is impossible from discs around isolated black holes in asymptotically flat spacetimes.[6]
- Strong collimation effect on jets escaping along the rotational axis of toroidal discs indicated by open equipotential surfaces that are narrowing strongly after crossing the static radius.

We can give to our results proper astrophysical relevance by presenting numerical estimates for observationally established current value of the RRCC[b]. Having the value of $\Lambda_0 \approx 1.3 \times 10^{-56} \mathrm{cm}^{-2}$, we can determine the mass parameter of the spacetime corresponding to any value of y, parameters of the equatorial circular geodesics and basic characteristics of both the thin and thick accretion discs (Ta-

---

[b]For more detailed information in the case of thick discs around Schwarzschild–de Sitter black holes see Ref. 13, where the estimates for primordial black holes in the early universe with a repulsive cosmological constant related to a hypothetical vacuum energy density connected with the electroweak symmetry breaking or the quark confinement are presented.

14   *Z. Stuchlík*

Table 1.   Mass parameter, the static radius and radius of the outer marginally stable orbit in extreme KdS black-hole spacetimes are given for the RRCC indicated by recent cosmological observations.

y	10^{-44}	10^{-34}	10^{-30}	10^{-28}	10^{-26}	10^{-22}
$M/M_\odot$	10	10^6	10^8	10^9	10^{10}	10^{12}
$r_{\rm s}/[\rm kpc]$	0.2	11	50	110	230	1100
$r_{\rm ms}/[\rm kpc]$	0.15	6.7	31	67	150	670

ble 1). Outer edge of the marginally bound thick accretion disc is determined by the outer marginally bound circular orbit which is located very close to, and for presented values of y almost at the static radius of a given spacetime.

It is well known[4] that dimensions of accretion discs around stellar-mass black holes ($M \sim 10M_\odot$) in binary systems are typically 10^{-3} pc, dimensions of large galaxies with central black-hole mass $M \sim 10^8 M_\odot$, of both spiral and elliptical type, are in the interval 50–100 kpc, and the extremely large elliptical galaxies of cD type with central black-hole mass $M \sim 3 \times 10^9 M_\odot$ extend up to 1 Mpc. Therefore, we can conclude that the influence of the RRCC is quite negligible in the accretion discs in binary systems of stellar-mass black holes as the static radius exceeds in many orders dimension of the binary systems. But it can be relevant for accretion discs in galaxies with large active nuclei as the static radius puts limit on the extension of the discs well inside the galaxies. Moreover, the agreement (up to one order) of the dimension of the static radius related to the mass parameter of central black holes at nuclei of large galaxies with extension of such galaxies suggests that the RRCC could play an important role in formation and evolution of such galaxies. Of course, the first step in confirming such a suggestion is modelling of the influence of the RRCC on self-gravitating accretion discs.

Acknowledgments

References

1. N. Bahcall, J. P. Ostriker, S. Perlmutter and P. J. Steinhardt, *Science* **284**, 1481 (1999).
2. E. W. Kolb and M. S. Turner, *The Early Universe* (Addison-Wesley, Redwood City, California, 1990), The Advanced Book Program.
3. D. N. Spergel *et al.*, *Astrophys. J. Suppl.* **148**, 175 (2003).
4. B. W. Carroll and D. A. Ostlie, *An Introduction to Modern Astrophysics* (Addison-Wesley, Reading, Massachusetts, 1996).
5. I. D. Novikov and K. S. Thorne, in *Black Holes*, eds. C. De Witt and B. S. De Witt (Gordon and Breach, New York–London–Paris, 1973), pp. 291–450.

6. M. Kozłowski, M. Jaroszyński and M. A. Abramowicz, *Astronomy and Astrophysics* **63**, 209 (1978).
7. M. A. Abramowicz, M. Jaroszyński and M. Sikora, *Astronomy and Astrophysics* **63**, 221 (1978).
8. Z. Stuchlík and S. Hledík, *Phys. Rev. D* **60**, 044006 (1999).
9. Z. Stuchlík and S. Hledík, *Acta Phys. Slovaca* **52**, 363 (2002).
10. M. A. Abramowicz and A. R. Prasanna, *Monthly Notices Roy. Astronom. Soc.* **245**, 720 (1990).
11. Z. Stuchlík and S. Hledík, *Classical Quantum Gravity* **17**, 4541 (2000).
12. S. Hledík, in *Gravitation: Following the Prague Inspiration (A Volume in Celebration of the 60th Birthday of Jiří Bičák)*, eds. O. Semerák, J. Podolský and M. Žofka (World Scientific, New Jersey, London, Singapore, Hong Kong, 2002), pp. 161–192.
13. Z. Stuchlík, P. Slaný and S. Hledík, *Astronomy and Astrophysics* **363**, 425 (2000).
14. L. Rezzolla, O. Zanotti and J. A. Font, *Astronomy and Astrophysics* **412**, 603 (2003).
15. M. A. Abramowicz, M. Calvani and L. Nobili, *Nature* **302**, 597 (1983).
16. F. de Felice and Y. Yunqiang, *Classical Quantum Gravity* **18**, 1235 (2001).
17. Z. Stuchlík and P. Slaný, *Phys. Rev. D* **69**, 064001 (2004).
18. D. R. Brill and S. A. Hayward, *Classical Quantum Gravity* **11**, 359 (1994).
19. S. A. Hayward and K.-I. Nakao, *Phys. Rev. D* **49**, 5080 (1994).
20. J. M. Bardeen and J. A. Petterson, *Astrophys. J. Lett.* **195**, L65 (1975).
21. B. Carter, in *Black Holes*, eds. C. De Witt and B. S. De Witt (Gordon and Breach, New York–London–Paris, 1973), pp. 57–214.
22. Z. Stuchlík, *Bull. Astronom. Inst. Czechoslovakia* **34**, 129 (1983).
23. J. Bičák, Z. Stuchlík and V. Balek, *Bull. Astronom. Inst. Czechoslovakia* **40**, 65 (1989).
24. Z. Stuchlík, *Bull. Astronom. Inst. Czechoslovakia* **31**, 129 (1980).
25. D. Lynden-Bell, *Nature* **223**, 690 (1969).
26. R. D. Blandford, in *Three hundred years of gravitation*, eds. S. W. Hawking and W. Israel (Cambridge University Press, 1987), p. 277.
27. M. Jaroszyński, M. A. Abramowicz and B. Paczyński, *Acta Astronom.* **30**, 1 (1980).
28. F. H. Seguin, *Astrophys. J.* **197**, 745 (1975).